Monitoring aquifer-system response to groundwater pumping and artificial recharge

John W. Bell,[1] Falk Amelung,[2] Alessandro Ferretti,[3] Marco Bianchi[3] and Fabrizio Novali[3*]
present a new satellite methodology for detecting and measuring long-term and seasonal aquifer-system response to pumping and recharge which potentially could be used for oil and/or gas reservoir monitoring.

In this study, we present results of a prototype study in Las Vegas Valley, Nevada. We have developed a series of velocity field maps of the valley for the 1992–1996, 1996–2000, and 2003–2005 time periods that show that, despite rising water levels associated with an artificial recharge programme, long-term, residual, inelastic aquifer-system compaction (subsidence) is continuing in several parts of the valley. In other areas, however, long-term subsidence has been arrested and locally reversed. The seasonal responses to alternating pumping and recharge cycles were segregated from the long-term trends and analyzed for spatial and temporal patterns. The results show oscillations in which the maximum seasonal responses are associated with the late stages of the annual artificial recharge cycles, and that similar seasonal subsidence signals are related to summer pumping cycles.

Purpose and scope

Many groundwater basins in the arid and semi-arid western US have experienced aquifer-system compaction, or subsidence, in response to heavy pumping. In this paper, we investigate aquifer system processes using a new remote sensing methodology that is becoming more and more common as a standard tool for measuring surface deformatio phenomena over large areas. The application of interferometric synthetic aperture radar (InSAR) studies to hydrogeological problems has advanced rapidly during the last decade, and it is now routinely applied to a wide range of groundwater resource issues, including groundwater flow modelling, estimation of aquifer-system hydraulic properties, and facilitating improved management of groundwater resources (Galloway and Hoffmann, 2006).

The application of permanent scatterer InSAR (PSInSAR) now provides an additional methodology that allows for greater resolution and accuracy in the detection of ground movement produced by aquifer system withdrawals and recharge. In this paper, we present results of a PSInSAR prototype study in Las Vegas Valley (Bell et al., 2008) that focuses on the pattern and timing of aquifer-system response to pumping and artificial recharge. We present a set of ground deformation maps that allow for a greater resolution in displacement time series than previously available through the use of conventional InSAR. Velocity and acceleration/deceleration analyses enable a close examination of patterns of subsidence and uplift responding to rising water levels during the study period.

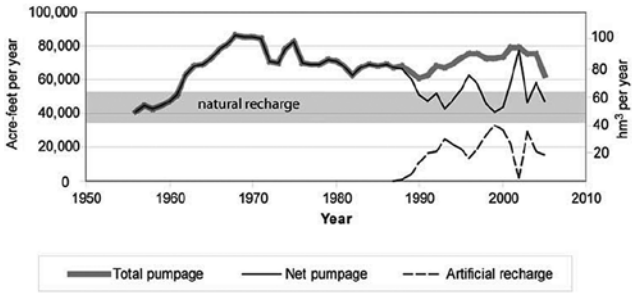

Figure 1 *Volume of total pumpage, artificial recharge, and net groundwater pumpage in Las Vegas Valley, 1950–2005. Artificial recharge programme begun by Las Vegas Valley Water District (LVVWD) in the late 1980s has resulted in reduced net pumpage each year, except for 2002. (Robert Coache, Nevada State Engineer's Office, unpub. data).*

The methodology

Conventional, differential, satellite repeat-pass InSAR is a methodology in which two radar scenes acquired over the same area at different times provide radar phase information that allows detection and measurement of sub-centimetre-scale ground movement in the form of a phase-change interferogram. The successful application of conventional InSAR to ground deformation studies is typically dependent upon a number of variables: availability of archival radar data to bracket the timing of the deformation event; suitable satellite baseline geometry; retrieval of coherent phase data, and identification and removal of phase changes unrelated to ground deformation, such as topography, residual satel-

[1] *Nevada Bureau of Mines and Geology, University of Nevada, Reno, Nevada, USA.*
[2] *Rosenstiel School of Marine and Atmospheric Science, University of Miami, Miami, Florida, USA.*
[3] *Tele-Rilevamento Europa, Via Vittoria Colonna, Milan, Italy.*
* *Corresponding author, E-mail: fabrizio.novali@treuropa.com.*

lite orbital errors, and atmospheric artifacts (cf., Hanssen, 2001). Measurement of the radar phase change is made on a pixel-resolution (~ 80 m^2) basis with a full-cycle of phase change equivalent to one-half of the radar wavelength (5.6 cm for C-band radar), or 2.8 cm of radar line-of-sight (LOS) displacement.

In contrast, the permanent scatterer (PS) methodology utilizes the identification and exploitation of individual radar reflectors, or permanent scatterers, that are smaller than the resolution pixel cell and that remain coherent over long time intervals in order to develop displacement time series (Ferretti et al., 2001). The resolution that is achieved by the identification of these PS targets effectively results in the creation of a data set consisting of many tiny 'benchmarks'. The advantages of the PS methodology are several: 1) good phase coherence is obtained from nearly all radar scenes regardless of geometrical baseline (perpendicular separation of the satellite positions), and long baseline interferometry with up to 1.6 km separation can be carried out; 2) all available radar scenes in the archive can be exploited; and 3) atmospheric phase contributions can be estimated and removed from the deformation phase signal.

A multi-interferogram approach, optimally incorporating more than 20 radar scenes, is used to identify consistently coherent targets throughout the entire time series, and to derive accurate phase-change data for each target. This is facilitated through the use of 'zero-baseline steering' which estimates the geometric phase contribution of different-baseline radar scenes and corrects this phase component relative to a reference or 'master' scene. The identification of stable scatterers is carried out by analyzing the time series of the radar amplitude values, and by looking for persistent, bright radar reflectors, most commonly fixed dihedral structures, such as buildings or other similar objects. False phase-change signals (artifacts) due to atmospheric contributions are estimated through the use of an atmospheric phase screen (APS) analysis. Atmospheric phase contributions are determined for each radar acquisition and subtracted from the total phase residuals derived from the interferometry process.

Approach

Two independent satellite data sets obtained from the European Space Agency were available for the study. We used 50 ERS-satellite acquisitions in a descending track mode taken over Las Vegas Valley between April 1992 and August 2000, and 19 ENVISAT-satellite acquisitions (all available ENVISAT acquisitions at the time of the study) in a descending track mode taken between October 2002 and May 2005 for the PS time series analyses. After APS estimation and correction to each acquisition, the two data sets were processed with the PSInSAR algorithm (Ferretti et al., 2001) to derive deformation phase data for each PS, to calculate the radar line-of-sight (LOS) displacement of each PS relative to the 'master' acquisitions (28 February 1997 for the ERS data and 27 February 2004 for the ENVISAT data), and to develop the average velocity fields from the two independent data sets. Because of the steep (~23°) look-angle for ERS and ENVISAT radar data, we assume that measured LOS displacements are vertical (cf., Hoffmann et al., 2001).

A 40 km x 40 km framework area containing 500,000 PS targets was initially analyzed (Figure 2). The areas exhibiting subsidence are visible in the Northwest Subsidence Bowl (NWSB) and along the north-south axis of the valley. The strong structural influence is very evident in this framework velocity field map, with the subsiding areas sharply bounded by faults, in good agreement with the earlier conventional InSAR results (Amelung et al., 1999; Hoffmann et al., 2001; Bell et al., 2002).

A 20 km x 20 km subset area containing 90,000 PS data points and centred over the NWSB-Eglington fault area was selected from the framework area to study in greater

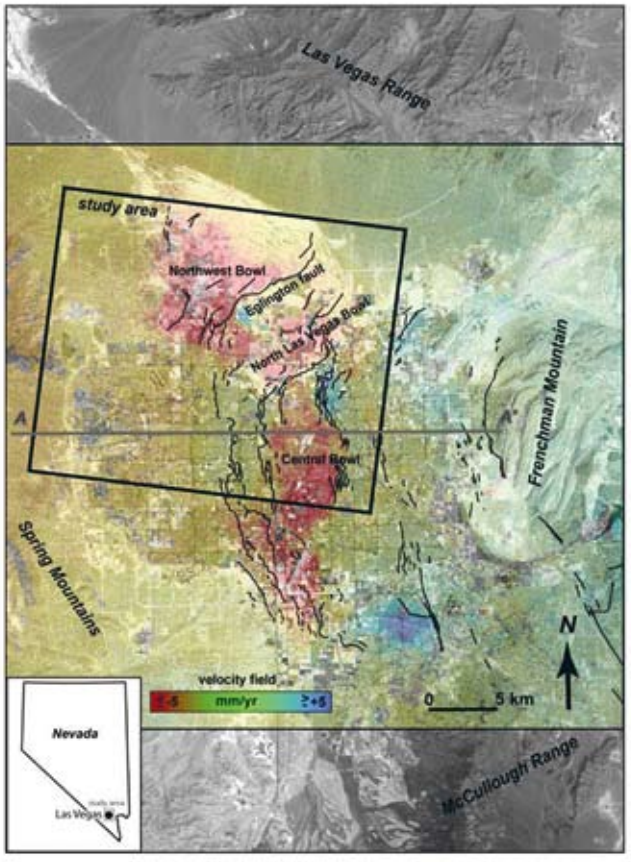

Figure 2 *Permanent scatterer velocity map of a 40 x 40 km framework area in Las Vegas Valley for the period 1996–2000 showing generalized PS rates; red areas denote subsidence and blue areas, uplift. Total number of PS targets in the framework area is more than 500,000. Study area (inset box) is a smaller subset (90,000 targets) of the PS data covering the northwest part of the valley.*

detail the aquifer-system response to temporal variations in groundwater pumping and artificial recharge (Figure 2). This area has exhibited the greatest subsidence since the 1960s, although the principal areas of groundwater pumping and recharge are located in the adjoining area to the south. Displacements for PS points in the Eglington fault area were determined, independent time series for the ERS and ENVISAT data sets were developed, non-linear motion of each time series (seasonal variation) was evaluated, and average displacement velocity maps were produced. Temporal windows were selected in order to examine subsidence trends occurring during the periods 1992–1996 (greatest subsidence rates), 1996–2000 (reduced subsidence rates), and 2003–2005 reduced subsidence rates with largest water-level recoveries). The temporal comparison further allowed the estimation of an acceleration field for the time period covered by the ERS data set. Because water levels in Las Vegas Valley exhibit large seasonal fluctuations, the time periods were selected to be consistent with seasonality. Individual PS time series were analyzed for seasonal and long-term trends to identify spatial patterns and to compare with water-level fluctuations.

Accuracy of the methodology

The accuracy of the PSInSAR methodology can be millimetre-scale if a sufficient number of acquisitions are utilized in the PS analysis (Ferretti et al., 2001). Owing to the large time gap between the two data sets in our study, ERS and ENVISAT acquisitions could not be efficiently co-processed, so separate time series were developed.

To test the accuracy of the PS results from Las Vegas Valley, we compared the results with independent vertical displacement data from a borehole extensometer operated by the US Geological Survey in the NWSB (Pavelko, 2000). Figure 3 shows a comparison between the 1995–2005 displacements recorded by the extensometer in the depth range of 4–244 m (total displacement 45 mm) and the PS time series data for an ERS target (DW197) and an ENVISAT target (BU292) adjacent to the extensometer (Figure 4a). Between 1995 and 2000, PS displacements replicate both the seasonal and long-term trends of the extensometer with an accuracy of about 3–5 mm, and the long-term average PS velocity and the compaction rates are very close: 4.6 mm/a and 5.0 mm/a, respectively. In a similar conventional InSAR test by Hoffmann et al. (2001), the seasonal displacements were found to be larger than the extensometer results, although the long-term InSAR trend was comparable to the extensometer record. They attributed the seasonal differences to compaction occurring below the 244m-depth of the extensometer.

Our comparison of the PS results and the extensometer record shows that while the long-term trends are also similar, we found less variation in the seasonal change

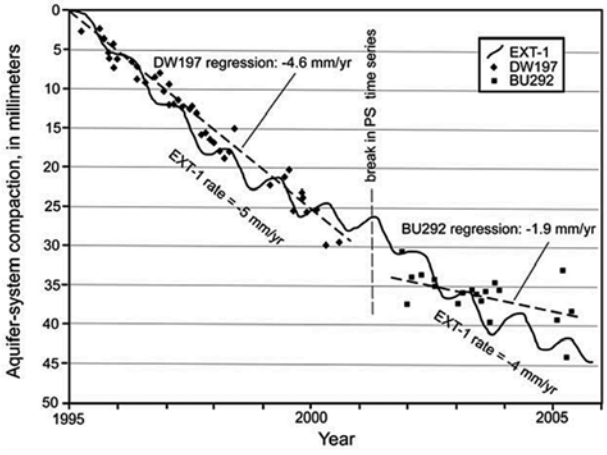

Figure 3 *Comparison of compaction recorded at US Geological Survey borehole extensometer EXT-1 (see Figure 4 for location) with permanent scatterer ERS results for 1995–2000 (PS target DW 197) and ENVISAT 2002–2005 (PS target BU 292). Because the two time series are processed separately, a break occurs between the ERS and ENVISAT data. Subsidence rates were calculated from average long-term trends of the extensometer records, and from linear regressions calculated for the PS data. (Extensometer data provided by M. Pavelko, US Geological Survey).*

than described by Hoffmann et al. (2001). The smaller ENVISAT data set shows more scatterers than the larger ERS data set, and the average 2002–2005 subsidence rate is lower than the extensometer compaction rate: 1.9 mm/a versus 4.0 mm/a, respectively. We regard the ENVISAT results as preliminary, containing greater uncertainties than the ERS results; the uncertainties of the ENVISAT data will improve as more acquisitions become available.

Results and discussion

Time series velocities and water-level change

The time series results were separated into three temporal windows in order to compare early ERS (1992–1996), late ERS (1996–2000), and recent ENVISAT (2003–2005) results with well-constrained water-level data for the same time periods (Figure 4). Quarterly water-level data provided by the Las Vegas Valley Water District for 1992–1996 (50 wells) and 1996–2000, 2003–2005 (100 wells) were used to produce water-level change maps for the study area. A comparison of the three temporal windows shows progressively reduced time series velocities (reduced subsidence rates) related to consistently rising water levels.

Between spring 1992 and spring 1996 (Figure 4a), subsidence in the NWSB occurred at a maximum average rate of 2–3 cm/a, consistent with earlier conventional InSAR interpretations and conventional geodetic data (Amelung et al., 1999; Bell et al., 2002). Water levels during this period rose by more than +10 m south of the subsidence bowl in the areas of artificial recharge, but continued to decline by as much as -5 m within the bowl, indicating that

the NWSB continued to be a zone of primary compaction. Between spring 1996 and spring 2000 (Figure 4b), average velocities in the NWSB had declined to 1–2 cm/a as water levels continued to rise by as much as +10 m, including within the NWSB. By the spring 2003 to spring 2005 period (Figure 4c), maximum subsidence rates in the NWSB had decreased to 5–10 mm/a, and all areas exhibited water level rise except for a newly developed area in the extreme northwest portion of the study area.

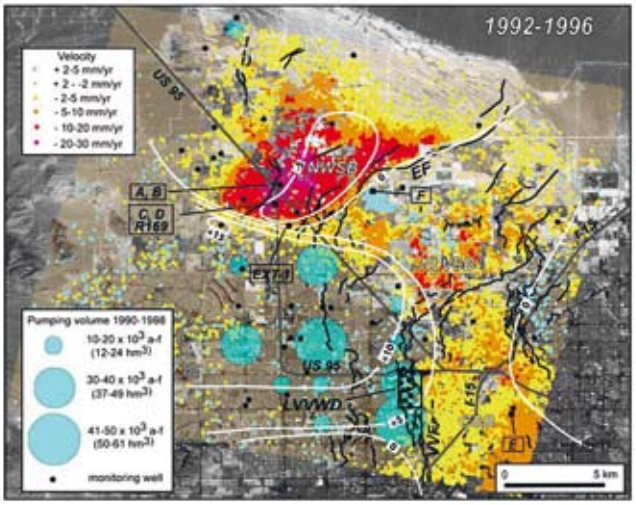

Figure 4a *Permanent scatterer velocity maps showing target velocities in mm/a for study area in the northwest portion of Las Vegas Valley. On all figures: NWSB (Northwest Subsidence Bowl); NLVSB (North Las Vegas Subsidence Bowl); CSB, (Central Subsidence Bowl); EF (Eglington fault); EXT-1 (Extensometer Location). Water-level change shown as white contours in metres, derived from water-level data points (black dots). Total PS target data set shown by light brown data points with values of -2 to +2 mm/a; PS targets discussed in Figure 5 identified by letters. Faults shown as black lines. (Water level data provided by the LVVWD/Southern Nevada Water Authority). (a) Permanent scatterer velocity map from ERS data for the period 21 April 1992 to 18 April 1996 and water-level change for the period March 1992 to April 1996. Total pumpage for 1990–1998 shown by light blue circles (pumping data provided by the Las VVWD/Southern Nevada Water Authority).*

The PS results show that the NWSB continued to be the most actively subsiding portion of the aquifer system as recently as 2005. Maximum subsidence rates in the NWSB prior to 1990 were in the order of 5 cm/a (Bell et al., 2002). The PS data show that these rates had decreased to less than 3 cm/a during the 1992–1996 period, and yet lower rates in subsequent years (see PS time series A, B, C and D in Figure 5).

The PS results also show that the aquifer-system response in the North Las Vegas bowl has been reversed, the only such area we have recognized to date. This area historically exhibited as much as 60 cm of subsidence . The PS data in the bowl show residual subsidence rates of more than 1 cm/a between 1996–2000 (PS target I; Figure 5). By 2003–2005, the residual subsidence had ceased and the area was undergoing aquifer-system uplift at a rate of as much as +1 cm/a (PS target J; Figure 5).

The combined 1992–1996–2000–2005 time series reflects a gradual decline in subsidence rates, a general observation that we have also made in earlier studies (Bell et al., 2002), but here clearly illustrated by diminishing velocities. On the basis of comparison of ERS velocity change between 1992–1996 and 1996–2000 for the same PS targets, an acceleration map (Figure 6) shows that aquifer-system compaction in the three principal subsidence bowls has been decelerating at an average rate of more than 1 mm/a^2. One small area in the northeast part of the study area has been accelerating.

Seasonal aquifer-system response

Most PS targets identified in the area of interest exhibit a seasonal signal superimposed on a long-term trend, includ-

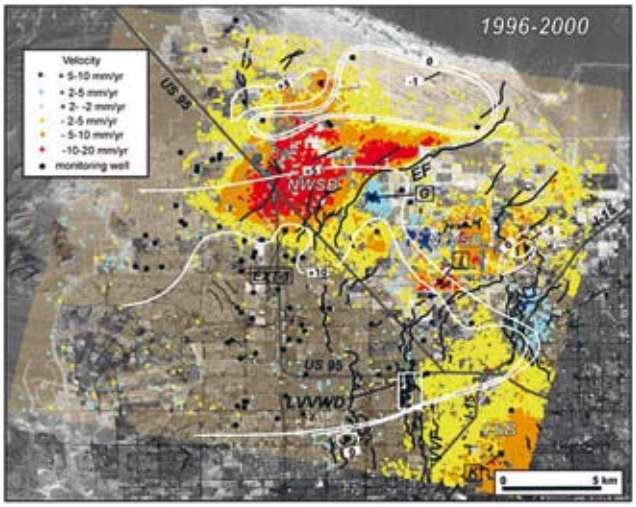

Figure 4b *Permanent scatterer velocity map from ERS data for the period 18 April 1996 to 28 April 2000 and water-level change for the period April 1996 to May 2000.*

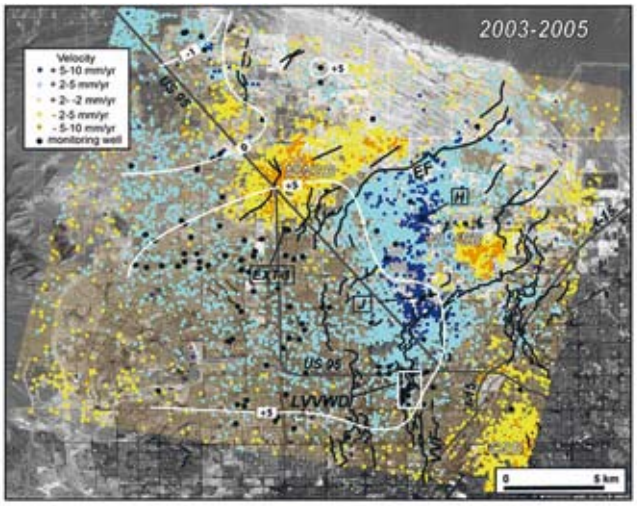

Figure 4c *Permanent scatterer velocity map from ENVISAT data for the period 18 April 2003 to 27 May 2005 and water-level change for the period April 2003 to May 2005.*

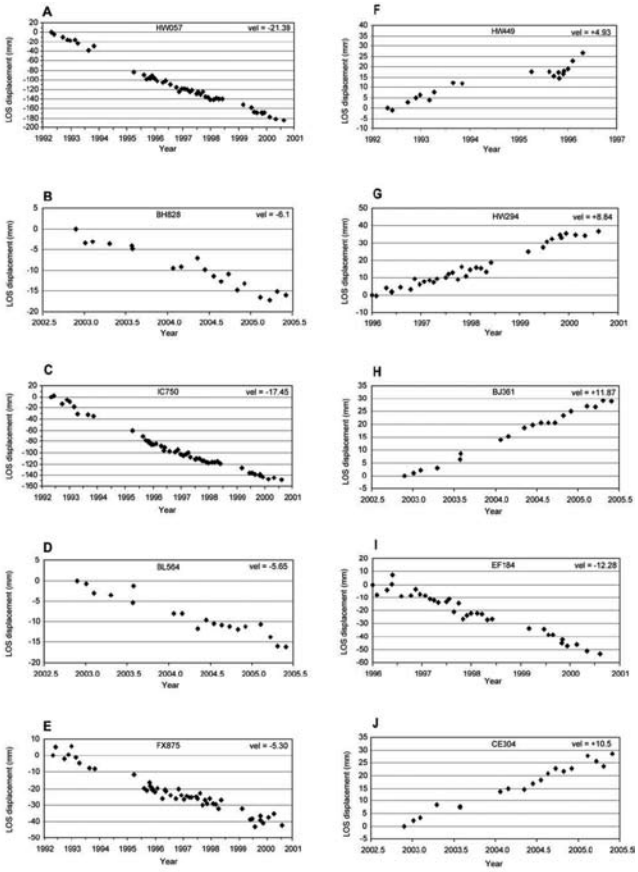

Figure 5 *PS time series for selected subsiding and uplifting data points (PS target name on each chart), with calculated average, long-term point velocities (mm/a) determined by linear regression of the time series. See Figures 4a, 4b for location of PS data points identified by charts A-J.*

ing the areas showing recovery and uplift (see Figure 5). In order to discern patterns of seasonal response, we segregated the seasonal signals by magnitude and time of year. To determine maximum seasonal amplitudes, we first subtracted the known, linear, long-term trend from each time series and then fit a sinusoidal model to each de-trended time series (Bell et al. 208):

$$Y(t) = Y_0 + Amp * \cos(2\pi(t - T))$$

where Amp is the maximum seasonal amplitude (mm) for either subsidence or uplift oscillations, T is time of year of the maximum amplitude, and Y_0 accounts for a constant shift in the model due to interferometric noise and artifacts. The linear trend (Figure 7a) is removed from the time series and a sinusoidal model is fit to the residual for each time series (Figure 7b). For the seasonal analysis we assume a one-year periodicity for the ground movement based on the annual cycles of pumping and recharge. The seasonal model was fit to each target in a 1995–1998 ERS data subset which contains the most robust seasonal data points. Each time series was first filtered by averaging all PS targets within a 500 m radius in order to reduce noise and to highlight areas of most active seasonal response. The model parameters were determined using a standard least mean squares estimation, and the results were then sorted by maximum amplitude (either subsidence or uplift) and time of year to look for spatial and temporal patterns.

The results show that the maximum seasonal response is clustered in four areas (Figure 8a). Area 1 is located at the northern margin of the NWSB near a spring zone; Area 2 is located immediately east of the LVVWD main well field; Area 3, which exhibits the largest seasonal amplitudes, is located in the CSB; and Area 4 is located at the eastern margin of the NLVSB adjacent to a new golf course. The reasons for the occurrence of these clusters and the spatial distribution are not entirely clear. On the basis of the location of the artificial recharge wells, only Area 2 adjacent to the LVVWD has a close spatial association with a recharge zone; the other clusters are 5–10 km from the nearest recharge well. However, Area 4 is adjacent to new golf course wells that began pumping in 1997 (Bruce Wert, written commun., 2007), and it is the only area that exhibits an acceleration in the subsidence rate (Figure 6). Each of these maximum seasonal amplitude clusters occurs in an area underlain by thick sections of fine-grained deposits (Plume, 1984; Morgan and Dettinger, 1996). Therefore we infer that the seasonal clusters are related to elastic response of sediments within the compressible aquitard sequence.

The maximum seasonal amplitude clusters in Areas 1, 2, and 3 occur during the January through March period of each year, indicating that a maximum seasonal oscillation is associated with the final stages of artificial recharge, which typically begins in late October and ends in late March of each year. In Area 2, a small cluster subset occurs

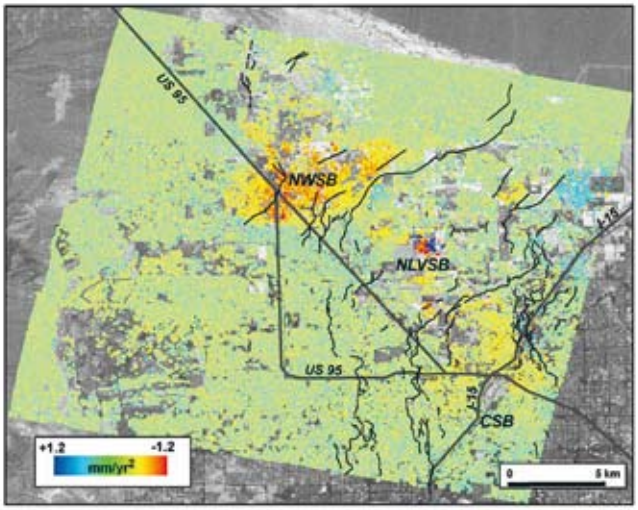

Figure 6 *Acceleration/deceleration map derived from comparison of 1992–1996 and 1996–2000 PS time series data. The NWSB exhibits residual subsidence that is decelerating at a rate of -1 mm/a2, while the NLVSB and the CSB are nearly stable. Faults shown in black.*

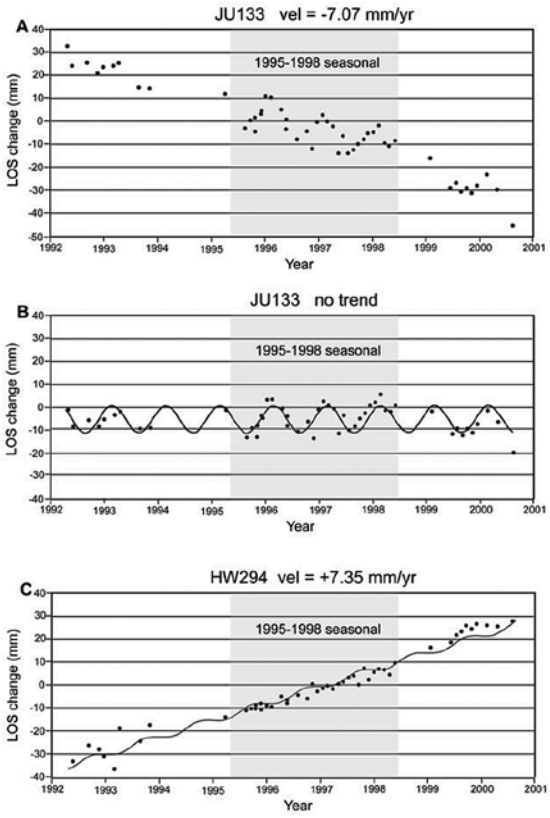

Figure 7 *Illustrative example of seasonal model application incorporating maximum seasonal amplitude and time of year for each PS target. (a) PS target JU133 time series for 1992–2000 showing linear subsidence trend of -7.07 mm/a; point K located on Figure 5b. (b) Seasonal sinusoidal model fit to target K time series results after removal of long-term subsidence trend. (c) Seasonal model fit to uplifting target G (Figures 4b, 5) showing seasonal uplift signal superimposed on long-term linear uplift of +7.35 mm/a.*

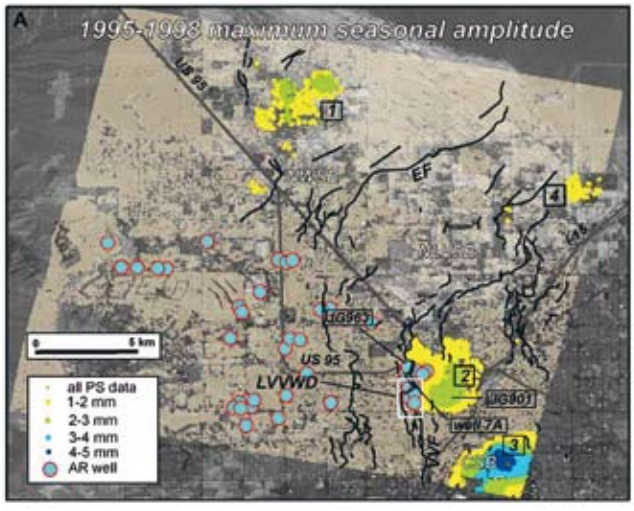

Figure 8 *Spatial and temporal clustering patterns of maximum seasonal amplitudes derived from application of seasonal sinusoidal model to all PS targets, after spatial filtering. Maximum seasonal amplitudes color-coded by size (mm). Four clusters (1, 2, 3, and 4) are present with the largest amplitudes located in cluster 3 in the CSB. Location of artificial recharge (AR) wells shown by blue circles. PS targets JG963 and JG901 occur on the west and east sides, respectively, of the VVF and well 7A is located within the LVVWD main well field.*

in early April at the actual end of the recharge period. It is interesting to note that Areas 1 and 3 are responding closely to seasonal recharge although spatially separated from the recharge wells, suggesting that elastic response to recharge is quite rapid throughout the aquifer system.

Seasonal signals are also superimposed on the larger uplift trends for some data points in the aquitard sequence (Figure 7c), indicating that there are both short- and long-term components to the elastic response. As the aquitards are expanding elastically due to long-term water-level recovery, they are also responding seasonally to annual pumping and recharge. As noted above, we speculate that the rapid seasonal response within the aquitard sequence may be due to the presence of fine-grained beds that respond like elastic aquifers. More advanced analyses based on aquifer modelling are described in Bell et al. (2008). The availability of PS data made it possible to calibrate the model and verify the correlation between aquifer system behaviour and surface displacements.

Conclusions

This study used the PSInSAR methodology together with detailed water-level change data to examine the temporal and spatial pattern of seasonal and long-term aquifer-system response to pumping and artificial recharge in Las Vegas Valley, providing insights into important aspects of the system response that can form the basis for similar studies in other heavily pumped groundwater basins.

This prototype study demonstrates that this is a robust, high-resolution, widely applicable methodology that improves upon conventional InSAR methodologies by providing the capability to more fully characterize temporal and spatial patterns of aquifer-system response. It could be further improved by increasing the sampling frequency and by combining data from different SAR viewing geometries and multiple satellites, thereby allowing greater resolution of annual fluctuations of the seasonal signals and detection of horizontal aquifer displacements.

We believe that this evolving methodology will provide an important new tool in future groundwater research and management that can be utilized in other heavily pumped groundwater basins throughout the western US and elsewhere. In addition, the permanent scatterer methodology may have broader applications to hydrologic research beyond groundwater resources, such as in the natural recharge in urban areas and in the system analyses of other ground fluid reservoirs. For example in oil and gas (Vasco and Ferretti, 2005), PSInSAR data can characterize reservoir processes such as fracture growth and volumetric changes based upon the surface deformations they generate, whether from primary or enhanced oil recovery techniques, or from CO_2 sequestration.

References

Amelung, F., D. L. Galloway, J. W. Bell, H. A. Zebker and R. J. Laczniak [1999] Sensing the ups and downs of Las Vegas: InSAR reveals structural control of land subsidence and aquifer-system deformation. *Geology*, **27**(6), 483–486.

Bell, J. W., F. Amelung, A. Ferretti, M. Bianchi and F. Novali [2008] Permanent scatterer InSAR reveals seasonal and long-term aquifer – system response to groundwater pumping and artificial recharge. *Water Resources Research*, Vol 44, W02407, doi: 10.1029/2007WR006152.

Bell, J. W., F. Amelung, A. Ramelli and G. Blewitt [2002] Land subsidence in Las Vegas, Nevada, 1935-2000: New geodetic data show evolution, revised spatial patterns, and reduced rates. *Env. Eng. Geosci.,* **VIII**(3), 155– 174.

Ferretti, A., C. Prati and C. Rocca [2001] Permanent scatterers in SAR interferometry. *IEEE Trans. Geosci. Remote Sens*., **39**(1), 8 –20.

Ferretti, A., G. Savio, R. Barzaghi, A. Borghi, S. Musazzi, F. Novali, C. Prati and F. Rocca [2007] Sub-millimeter accuracy of InSAR time series: Experimental validation. *IEEE Trans. Geosci. Remote Sens*., **45**(5), 1142–1153.

Galloway, D. L. and J. Hoffmann [2006] The application of satellite differential SAR interferometry-derived ground displacements in hydrogeology. *Hydrogeol. J.,* doi:10.1007/s10040-006-0121-5.

Hanssen, R. [2001] *Radar interferometry, Vol 2: Remote sensing and digital image processing*. Kluwer Academic Publishers, Dordrecht, Boston, London. 308 pp.

Hoffmann, J. and H. A. Zebker [2003] Prospecting for horizontal surface displacements in Antelope Valley, California, using satellite radar interferometry. *J. Geophys. Res*., **108**(F1), 6011, doi:10.1029/2003JF000055.

Hoffmann, J., H. A. Zebker, D. L. Galloway and F. Amelung [2001] Seasonal subsidence and rebound in Las Vegas Valley, Nevada, observed by synthetic aperture radar interferometry. *Water Resour. Res*., **37**(6), 1551–1566.

Las Vegas Valley Water District [2005] 2005 Artificial recharge annual report. *Las Vegas Valley Water Disrict*. Unpublished report, 150 pp.

Morgan, D. S., and M. D. Dettinger [1996] Groundwater conditions in Las Vegas Valley, Clark County, Nevada, Part 2: Hydrogeology and simulation of groundwater flow. *US Geological Survey,* Water Supply Paper 2320-B, 124 pp.

Pavelko, M. T. [2000] Ground water and aquifer-system compaction data from the Lorenzi Site, Las Vegas, Nevada, 1994-1999. *US Geological Survey,* Open-file Report 00-362, 26 pp.

Plume, R. W. [1984] Ground-water conditions in Las Vegas Valley, Clark County, Nevada. *US Geological Survey,* Open-file Report 84-130, 25 pp.

Vasco, D.W. and A. Ferretti [2005] On the use of quasi-static deformation to understand reservoir fluid flow. *Geophysics*, **70**(4), 13-27.